Journal of Materials Chemistry A

Accepted Manuscript

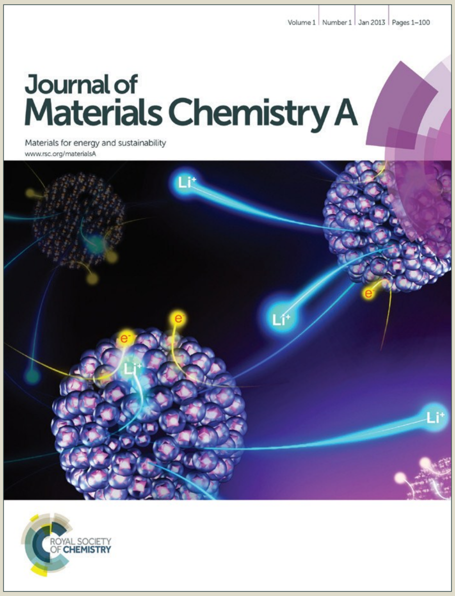

Volume 1 | Number 1 | Jan 2013 | Pages 1–100

Journal of Materials Chemistry A

Materials for energy and sustainability

www.rsc.org/materialsA

ROYAL SOCIETY OF CHEMISTRY

www.rsc.org/materialsA

Journal Name

COMMUNICATION

Highly Efficient Polyoxometalate-based Catalysts for Clean-Gasoline Synthesis

Received 00th January 20xx,
Accepted 00th January 20xx

DOI: 10.1039/x0xx00000x

www.rsc.org/

Chunling Wang,[a] Cheng Liu,[a] Yunhang Hu,[b] Xianni Bu,[c] Tiejun Zhao,[c] Kuochih Chou[a] and Qian Li*[a,d]

Poor selectivity for gasoline products is a critical issue for Fischer-Tropsch synthesis (FTS). Herein, we report that the introducion of polyoxometalates $Cs_{2.5}H_{0.5}PW_{12}O_{40}$ (CsPW) into conventional FTS catalyst (Co/Al_2O_3) can create a highly efficient bifunctional catalyst, leading to 118% increase in the selectivity of gasoline. Furthermore, it was found that such a significant improvement is due to the effective hydrocracking of havier hydrocarbon products at CsPW sites.

The high quality of diesel and gasoline fuel is required to reduce air pollution. Fischer-Tropsch synthesis (FTS) is an important industrial process for clean hydrocarbon fuels through syngas from non-petroleum carbon resources such as natural gas, shale gas, coal, or biomass[1]. Over conventional FTS catalysts, the hydrocarbon products generally follow the unselective Anderson-Schulz-Flory (ASF) distribution from C_1 to C_{100}[2-4]. To obtain gasoline ($C_5 \sim C_{12}$), the heavier products need to be further hydrocracked and isomerized to light and/or branched hydrocarbons, in which the acidity of the catalyst is crucial[5]. Acidic zeolites are widely used as catalyst supports or co-catalysts to increase the selectivity of gasoline or diesel in one- step process[6-11]. However, the strong acidity of zeolites might also cause the over-cracking of hydrocarbon products[6].

Polyoxometalates (POMs) comprise a large class of nanosized, polynuclear metal-oxo anions being formed by early transition metal ions (V, Nb, Ta, Mo, W) in high oxidation states[12-14]. As a typical polyoxoanion with unique properties[15-17], POMs could meet the requirement for tuning the selectivity of FTS products. They possess suitable acidity[18-20], which would be efficient for the hydrocracking of heavier FTS products. Furthermore, their acidic properties could be easily tuned by simple synthetic routes, such as embedding metal ions in their structures[21, 22].

Tungstophosphoric acid ($H_3PW_{12}O_{40}$) is one of the strong acidic compound which has been used as an efficient catalyst in various reactions[23, 24]. Partial substitution of protons by Cs^+ could adjust the insolubility and the amount of available surface acid sites. The 2.5 Cs^+ substituted sample, $Cs_{2.5}H_{0.5}PW_{12}O_{40}$ (CsPW) has been demonstrated to possess sufficient higher thermal-stability and acidity than the parent acid $H_3PW_{12}O_{40}$[25, 26], which can serve as heterogeneous catalysts for hydrocracking/hydroisomerization reactions associated with Fischer-Tropsch processes[27]. So far, however, the direct utilization of POMs for a FTS process has not been explored. Herein, we report efficient bifunctional FTS catalyst (P-F) consisting of the insoluble POMs ($Cs_{2.5}H_{0.5}PW_{12}O_{40}$) and conventional FTS catalyst (Co/Al_2O_3) for the FTS process, which exhibited a high selectivity for C_5-C_{12} gasoline.

CsPW (Fig.1a) samples were synthesized using a solid approach (followed by calcination for two hours) which can easily control the mole ratio of precursors $H_3PW_{12}O_{40}$ and $CsNO_3$ as described in literature[28, 29]. Furthermore, the samples were subjected to thermal and structure characterizations. In the thermogravimetric analysis, no obvious weight loss was observed in the temperature range of 473 to 573 K (Fig.S1). The range covers special temperatures, including 473 K (syngas flow to catalyst), 493 K (the FTS reaction generally occurred), 523 K (produce gasoline), and 573 K (metal oxide Co_3O_4 could be reduced to active metal Co). The IR spectra of the samples showed four characterization absorption bands of the Keggin unit at 1080, 989, 889, and 805 cm^{-1}, which could assign to υ_{as}(P-O-W),

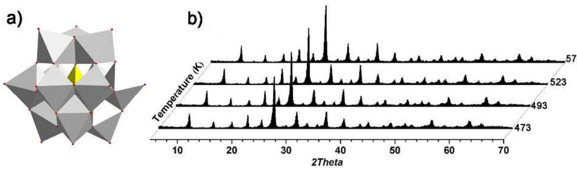

Fig.1. (a) The polyanion structure of CsPW with the represented by polyhedra. Colour codes: W grey, P yellow, O red; (b) XRD patterns of CsPW from 473K to 573K.

---

[a] State Key Laboratory of Advanced Special Steels, Shanghai University, Shanghai 200072, P. R. China. E-mail: shuliqian@shu.edu.cn
[b] Department of Materials Science and Engineering, Michigan Technological University, Houghton, Michigan, 49931, USA
[c] CAS Key Laboratory of Low-Carbon Conversion Science and Engineering, Shanghai Advanced Research Institute, Chinese Academy of Sciences, Shanghai 201210, P. R. China.
[d] Institute of Genomic Material, Shanghai University, Shanghai 200444, P. R. China

Electronic Supplementary Information (ESI) available: Experimental details and characterization techniques such as TG, IR, H_2-TPR, XRD, and FTS results (Fig.S1-8). See DOI: 10.1039/x0xx00000x

υ_{as}(W-O$_t$), υ_{as}(W-O$_c$-W), and υ_{as}(W-O$_e$-W) vibrations[30], respectively. The absorption bands remained almost unchanged with increasing temperature up to 773 K (except some decrease of the peak intensities) (Fig.S2). This indicates that the primary structure (Keggin unit structure) of CsPW is stable at a temperature below 773 K. Furthermore, the XRD patterns of CsPW samples (Fig.1b) exhibit all reflections corresponding to a cubic P_{n3m} crystalline structure, similar with other literature data[21, 22]. This confirms that the secondary structure of the CsPW is stable in the temperature range from 473 to 573 K.

Bifunctional catalysts (P-F) with four CsPW contents (*i.e.* 5%, 10%, 20%, and 50%), which were prepared by ball milling, are denoted as 0.05P-F, 0.10P-F, 0.20P-F, and 0.50P-F, respectively. As shown in Table 1, one can see that the measured bulk weights of W element are close to their theoretical values. Furthermore, XRD measurements showed that the bifunctional catalyst consists of Co_3O_4 and CsPW (Fig.2a, Fig.S3). The crystallite sizes of Co_3O_4, which were calculated from the diffraction peak at $2\theta = 59.5$ using Scherrer equation, increased with increasing CsPW amount (Table 1). That indicates the size of Co_3O_4 in P-F modest increased with the increase amount of CsPW. The H_2-TPR profiles of the bifunctional catalysts were obtained. As shown in Fig.S4, one can see three H_2 consumption peaks for Co/Al_2O_3, 0.05P-F, 0.10P-F, and 0.20P-F samples and a more complicated TPR curve for 0.50P-F sample. Co/Al_2O_3 catalyst exhibits two peaks at 443 K and 513 K, which are associated with the reduction of Co_3O_4 to CoO and the transformation of CoO to Co, respectively. The peak at a higher temperature (about 733 K) indicates that some Co oxide species are much more difficult to be reduced probably due to the strong metal-support interaction between Co and Al_2O_3 in some phases (such as $CoAl_2O_4$). The consumption of H_2 at temperature below 673 K decreased with increasing CsPW, indicating that CsPW decreased the cobalt oxide reducibility. This is probably due to the strong interaction between the Cs ions and the cobalt species[31, 32]. For the catalyst 0.50P-F, the large reduction peaks at about 823 and 1043 K indicate the reduction of some W^{VI} species.

The acidity of the bifunctional catalysts was evaluated by ammonia temperature-programmed desorption (NH_3-TPD) (Fig.2b). The CsPW exhibits three desorption peaks in the NH_3-TPD profile, corresponding to the weak, medium-strength, and strength acid sites. For the CsPW, the higher temperature peak (observed at about 843 K) can be attributed to the strong Brønsted acid sites. Two NH_3 desorption peaks were observed for the bifunctional catalysts at 343 and 523 K. For Co/Al_2O_3, three peaks at 313-383 K, which are associated with weaker acid sites, was observed. This indicates that the acidity of Co/Al_2O_3 is significantly weaker than that of the bifunctional catalyst. The strength of the acid site increases with increasing CsPW. As a result, for the bifunctional catalyst, the heavier hydrocarbons can be hydrocracked at the strong acidic sites of CsPW, while the active metal Co sites are responsible for the syngas conversion to linear hydrocarbons (Scheme 1).

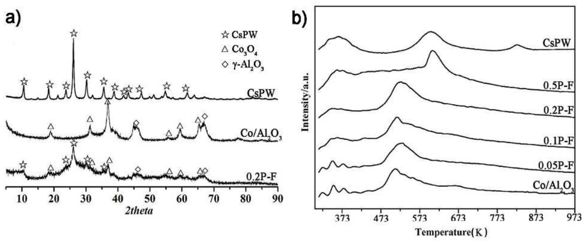

Fig.2. (a) XRD pattern of CsPW, Co/Al_2O_3 and 0.20P-F; (b) NH_3-TPD profiles of bifunctional catalysts.

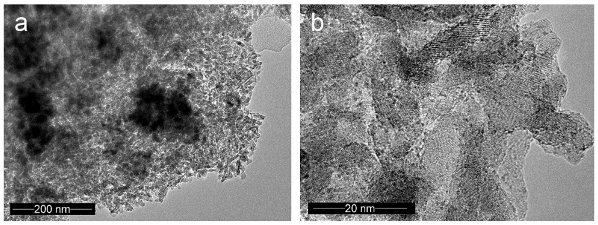

Fig.3 (a) The TEM image of the Co_3O_4 particles in the catalysts 0.2P-F; (b) The TEM image shows the dispersed CsPW particles on the catalysts 0.2P-F.

The pore-size distribution curves, which were obtained from the N_2 adsorption-desorption isotherms using the Barrett-Joyner-Halenda (BJH) method, showed the mesoporous structure of the bifunctional catalysts (Figs.S5 and S6). Compared with the model FTS catalyst Co/Al_2O_3 (123.7 $m^2 \cdot g^{-1}$), the bifunctional catalysts exhibited the obvious decrease in surface area and pore volume, particularly for the sample 0.5P-F (remarkably decrease to 73.5 $m^2 \cdot g^{-1}$). That happened because CsPW particles entered into the pores of Co/Al_2O_3, reducing the pore volume. This was confirmed by the TEM images (Fig.3), which clearly showed that the CsPW particles were located in the mesopores of the γ-Al_2O_3 support and well dispersed in 0.20P-F samples with an average size of ca. 0.4 nm (Fig.3b). However, the average particle size of Co_3O_4 is 13.5 nm, which is much larger than the particle size of CsPW. The mapping of the element P, Cs and W further revealed the high dispersion of CsPW (Fig.S7). The well-dispersed CsPW on the FTS catalyst created highly-dispersed acidic sites in the bifunctional catalyst. In other words, the ball milling constitutes an efficient approach to disperse the CsPW on FTS catalyst. The excellent contact between the CsPW and the FTS catalyst (Co/Al_2O_3) ensures that heavy hydrocarbons generated over Co/Al_2O_3 can be easily captured and then hydrocracked by the CsPW. Such an in-situ hydrocracking can be expected to increase the selectivity of gasoline products. This was confirmed by the following catalytic performance tests.

The performance of the bifunctional catalysts was tested for FTS using a fixed-bed reactor and the results are listed in Table 1. For all catalysts, the reaction reached a steady state within 6 hours and then CO conversion remained unchanged. For FTS catalyst (Co/Al_2O_3) without CsPW, one can see the typically ASF distribution of products, which is wide and unselective from C_1 to C_{50}^+ hydrocarbons (Fig.4a and 4b). In contrast, the introduction of CsPW into the FTS catalyst led to a remarkable improvement of C_5-C_{12}

Scheme 1 The reaction mechanism of bifunctional catalyst consist of FTS catalyst and polyoxometalates

Table 1 Effect of CsPW amount on C_5-C_{12} selectivity

Catalyst	CsPW (wt%)	CsPW content (wt%)^a	S_{BET} (m^2/g)	D_{pore} (nm)	V_{pore} (cm^3/g)	Particle size(nm) XRD	CO conv. (%)	Selectivity (%)					
								CH_4	CO_2	C_2-C_4	C_5-C_{12}	C_{13}-C_{20}	≥C_{21}
Co/Al_2O_3	-	-	123.7	12.1	0.41	7.5	84.0	12.6	0	8.2	21.3	27.2	30.7
0.05P-F	5	4.97	118.5	8.8	0.26	7.6	85.1	13.3	2.1	16.9	34.2	22.2	11.3
0.10P-F	10	10.15	110.2	9.7	0.25	7.9	85.3	15.7	3.7	14.4	42.4	20.6	3.1
0.20P-F	20	19.93	110.4	10.3	0.28	8.3	82.7	14.5	3.7	13.7	46.4	19.1	2.8
0.50P-F	50	50.32	73.5	10.5	0.18	8.7	77.9	16.5	3.5	10.0	39.3	23.7	7.0

Reaction conditions: $H_2/CO = 2:1$, SV = 6000h^{-1}, P = 2.0 MPa, Co/Al_2O_3 catalyst 0.5 g, 523K, 72h. CsPW content was calculated based on W element.

selectivity (Fig.4a and 4b), namely, the C_5-C_{12} products increased from 21.3 to 46.4% by adding 20wt% CsPW into the FTS catalyst, which was accompanied by only slight decrease in the CO conversion (the average CO conversion of 0.20P-F catalyst remained as high as 82.7%). This indicates that the selectivity of gasoline (C_5-C_{12}) was increased by 118%.

The effect of CsPW content (from 0 to 50 wt%) on the C_5-C_{12} selectivity was examined at 523K (Fig.4c and Table 1). The C_{21}^+ products decreased significantly from 30.7 to 2.8% with increasing CsPW from 0 to 20 wt% (Fig.4d). Such a decrease in C_{21}^+ products with the increase of C_5-C_{12} selectivity over the bifunctional catalyst indicates that C_{21}^+ hydrocarbons was hydrocracked by acid sites of CsPW. The results are better than those reported for zeolite at similar reaction conditions[6, 11]. This indicates that the relatively strong acidity of the POMs is beneficial to the selective production of gasoline. However, the C_{21}^+ selectivity went up to 7% when the CsPW content increased to 50 wt%, leading to a relatively low CO conversion (77.9%) and high CH_4 selectivity (16.5%) over 0.5P-F catalyst. It is generally recognized that the FTS activity is mainly dependent on the number of exposed cobalt atoms. The low conversion of CO over 0.5P-F catalyst can be explained as follows: since CsPW content is large, some of the CsPW possess the pores of Co/Al_2O_3 and thus cover some of exposed cobalt surface area, which prevented syngas molecules from contacting with Co active metals. The selectivity for CO_2 over 0.10P-F, 0.20P-F, and 0.50P-F catalysts is 3.5-3.7%, which is much larger than that over Co/Al_2O_3 catalyst without CsPW. This suggests that the acidity of CsPW enhanced CO dissociation and promoted the water-gas shift reaction.

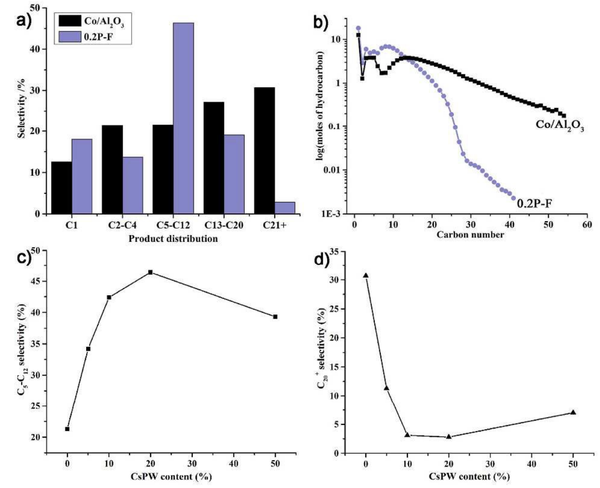

Fig.4. (a) Hydrocarbon selectivity for Co/Al_2O_3 and the bifunctional catalyst 0.2P-F; (b) ASF distribution of products for catalysts 0.2P-F and Co/Al_2O_3; (c) Effect of CsPW content on C_5-C_{12} selectivity; (d) Effect of CsPW content on C_{21}^+ selectivity.

Finally, IR spectra revealed that the Keggin type structure of CsPW was stable in the FTS reaction. As shown in Fig.S8, one can see four feature peaks (of Keggin type structure) at 804, 888, 985, 1075 cm^{-1} indicating that the primary structure of CsPW remained in the used 0.20P-F-spent catalyst. However, the other two main bands of the used catalyst at 2846 cm^{-1} and 2907 cm^{-1} are associated with the C-H and C-C band vibrations. This is properly due to the hydrocarbon products retained in the pore of the catalyst.

In conclusion, a highly efficient bifunctional catalyst was successfully synthesized by introducing CsPW into conventional FTS catalyst Co/Al_2O_3 for gasoline (C_5-C_{12}) production from syngas via FTS reaction. The C_5-C_{12} production reaches about 44.6% over the bifunctional catalyst, which is significantly larger than the maximum value (ca. 21.3%) over a conventional FTS catalyst. The unique acidic property of POMs plays an important role in the selectivity enhancement. Compared to Fe-based high-temperature Fischer-Tropsch (>573K) for gasoline-range hydrocarbons, POMs based bifunctional catalyst consume less energy and possess relatively high CO conversion and less CO_2 selectivity[33-35]. But there are still two disadvantages of the POMs based catalyst for the FTS process. Firstly, the gasoline selectivity is still need to be enhanced. In our resent research, we use POMs promote Ru based FTS catalyst to obtain higher gasoline selectivity. Secondly, the isomerization of the C_5-C_{12} over POMs based catalyst was not as highly as the zeolite based catalyst. The element composition (such as added Al or Ga elements) and the type of POMs (using the lacunary POMs or other type such as Wells-Dawson type POMs) could be changed to enhance the extent of isomerization.

We gratefully acknowledge the financial support from the National Natural Science Foundation of China (No.21201122, No.51222402) and “ShuGuang” project supported by Shanghai Municipal Education Commission and Shanghai Education Development Foundation (13SG39).

Notes and references

1. A. Steynberg and M. Dry, *Fischer-Tropsch Technology*, Elsevier, 2004.
2. G. P. Van der Laan and A. Beenackers, *Catal. Rev.: Sci. Eng.*, 1999, 41, 255-318.
3. A. Y. Khodakov, W. Chu and P. Fongarland, *Chem. Rev.*, 2007, 107, 1692-1744.
4. Y. Liu, I. Florea, O. Ersen, C. Pham-Huu and C. Meny, *Chem. Commun.*, 2015, 51, 145-148.
5. J. R. Rostrup-Nielsen, *Science*, 2005, 308, 1421-1422.
6. J. Bao, J. He, Y. Zhang, Y. Yoneyama and N. Tsubaki, *Angew. Chem. Int. Ed.*, 2008, 47, 353-356.
7. Q. Zhang, J. Kang and Y. Wang, *Chemcatchem*, 2010, 2, 1030-1058.
8. J. Kang, K. Cheng, L. Zhang, Q. Zhang, J. Ding, W. Hua, Y. Lou, Q. Zhai and Y. Wang, *Angew. Chem. Int. Ed.*, 2011, 50, 5200-5203.
9. X. Peng, K. Cheng, J. Kang, B. Gu, X. Yu, Q. Zhang and Y. Wang, *Angew. Chem. Int. Ed.*, 2015, 54, 4553-4556.
10. C. Xing, G. Yang, M. Wu, R. Yang, L. Tan, P. Zhu, Q. Wei, J. Li, J. Mao, Y. Yoneyama and N. Tsubaki, *Fuel*, 2015, 148, 48-57.
11. C. Xing, W. Shen, G. Yang, R. Yang, P. Lu, J. Sun, Y. Yoneyama and N. Tsubaki, *Catal. Commun.*, 2014, 55, 53-56.
12. M. T. Pope and A. Müller, *Angew. Chem. Int. Ed.*, 1991, 30, 34-48.
13. U. Kortz and T. Liu, *Eur. J. Inorg. Chem.*, 2013, 1559-1560.
14. A. Banerjee, B. S. Bassil, G.-V. Roeschenthaler and U. Kortz, *Chem. Soc. Rev.*, 2012, 41, 7590-7604.
15. N. Mizuno, C. Nozaki, I. Kiyoto and M. Misono, *J. Am. Chem. Soc.*, 1998, 120, 9267-9272.
16. N. Mizuno and M. Misono, *Chem. Rev.*, 1998, 98, 199-217.
17. M. Sun, J. Zhang, P. Putaj, V. Caps, F. Lefebvre, J. Pelletier and J.-M. Basset, *Chem. Rev.*, 2014, 114, 981-1019.
18. W. Knaeble, R. T. Carr and E. Iglesia, *J. Catal.*, 2014, 319, 283-296.
19. K. Inumaru, T. Ishihara, Y. Kamiya, T. Okuhara and S. Yamanaka, *Angew. Chem. Int. Ed.*, 2007, 46, 7625-7628.
20. W. Alharbi, E. Brown, E. F. Kozhevnikova and I. V. Kozhevnikov, *J. Catal.*, 2014, 319, 174-181.
21. V. Sasca, L. Avram, O. Verdes and A. Popa, *Appl. Surf. Sci.*, 2010, 256, 5533-5538.
22. K. Narasimharao, D. Brown, A. Lee, A. Newman, P. Siril, S. Tavener and K. Wilson, *J. Catal.*, 2007, 248, 226-234.
23. N. V. Maksimchuk, K. A. Kovalenko, S. S. Arzumanov, Y. A. Chesalov, M. S. Melgunov, A. G. Stepanov, V. P. Fedin and O. A. Kholdeeva, *Inorg. Chem.*, 2010, 49, 2920-2930.
24. J. C. Yori, J. M. Grau, V. M. Benitez and J. Sepulveda, *Appl. Catal. A-Gen.*, 2005, 286, 71-78.
25. X. K. Yang, L. F. Chen, J. A. Wang, L. E. Norena and O. Novaro, *Catal. Today*, 2009, 148, 160-168.
26. Y. Liu and M. Misono, *Materials*, 2009, 2, 2319-2336.
27. Y. Liu, K. Murata and K. Sakanishi, *Fuel*, 2011, 90, 3056-3065.
28. L. Zhang, B. Yue, Y. Ren, X. Chen and H. He, *Catal. Sci. Technol.*, 2013, 3, 2113-2118.
29. Y. Zou, B. Yue, B. Zhang and H. Y. He, *Chem. Lett.*, 2006, 35, 202-203.
30. S. M. Choi, Y. Wang, Z. M. Nie, J. Liu and C. H. F. Peden, *Catal. Today*, 2000, 55, 117-124.
31. A. H. Lillebo, E. Patanou, J. Yang, E. A. Blekkan and A. Holmen, *Catal. Today*, 2013, 215, 60-66.
32. O. Borg, N. Hammer, B. C. Enger, R. Myrstad, O. A. Lindvag, S. Eri, T. H. Skagseth and E. Rytter, *J. Catal.*, 2011, 279, 163-173.
33. R. M. M. Abbaslou, A. Tavassoli, J. Soltan and A. K. Dalai, *Appl. Catal. A-Gen.*, 2009, 367, 47-52.
34. Z. Yang, S. Guo, X. Pan, J. Wang and X. Bao, *Energ. Environ. Sci.*, 2011, 4, 4500-4503.
35. Q. Zhang, W. Deng and Y. Wang, *J. Energ. Chem.*, 2013, 22, 27-38.

Graphical Abstract:

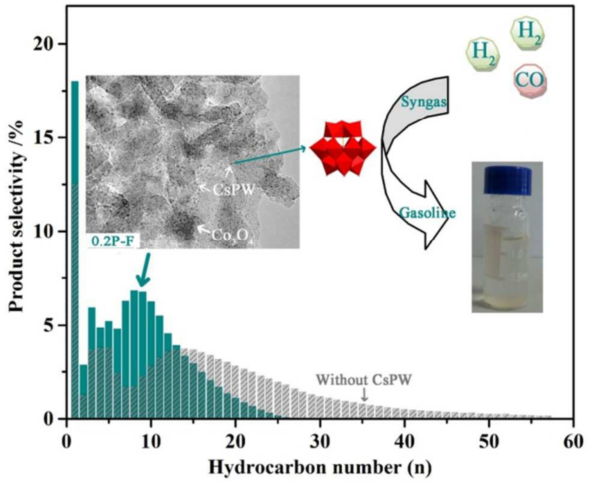

The introducing of CsPW into Co/Al_2O_3 leads to 118% increase in the selectivity of gasoline.